MICROSTRUCTURE AND MECHANICAL PROPERTIES OF FSLA STEEL PRODUCED BY METAL INJECTION MOLDING

Lane Donoho and Dwight Webster
Advanced Metalworking Practices, LLC
Carmel, IN 46032

Chris Schade and Tom Murphy
Hoeganaes Corporation
Cinnaminson, NJ 08077

ABSTRACT

An alloy, called FSLA (free-sintering low-alloy), was designed and implemented for use with binder jet printing, however the powder is also suitable for metal injection molding. This work focuses on examining the mechanical properties and microstructure of the FSLA alloy and its response to standard metal injection molding processes. The work also reviews the various heat treatments that can be utilized with the alloy to produce a range of properties for various applications. The microstructure and mechanical properties will be compared to the same alloy that has been produced by the AM process of binder jetting.

INTRODUCTION

The characteristics of powder used for Metal Binder Jetting (MBJ) are very similar to those used for metal injection molding (MIM). Both technologies require fine powder (typically with a d_{90} less than 25 micrometers) that are free flowing. Both technologies also require a powder that is spherical, leading to high apparent and tap densities. For MBJ, the spherical powders are necessary to ensure that, as they are spread in the build bed, they flow easily and therefore achieve a high density in the bed. For MIM, the spherical nature of the powders helps the loading level that can be achieved in the binder/powder feedstock, leading to high densities in the molded part. The surface area of the very fine powders is essential to achieve adequate densities during the sintering process. Therefore, it is logical that powders developed for one technology may be suitable for the other. In addition, the binders utilized by both technologies often interact with the powder surface, complicating the sintering process and requiring additional development efforts on the part of the end user. In previous papers an alloy called FSLA (Free Sintering Low Alloy) was introduced for MBJ, which was comparable in properties to a wrought grade of steel called DP600 [i.e. Ultimate Tensile Strength (UTS) = 600 MPa].[1] Unlike other low alloys steels, the chemistry of the FSLA alloy was tailored to have a mixed microstructure of approximately 50 volume percent ferrite and 50 volume percent austenite at the sintering temperatures. Work by previous authors suggested the increase in grain boundary area between the austenite and ferrite would increase the diffusion and lead to higher sintered densities.[2-3]

This was proven to be the case as the MBJ-FSLA had superior sintered density than other low alloy steels. The ferrite stabilizing elements (chromium, molybdenum and silicon) were all chosen because of their hardenability characteristics which, allowed for the transformation of the austenite to martensite at moderate cooling rates. The alloy chemical composition allowed for intercritical annealing in a two-phase region of austenite and ferrite. With an appropriate cooling rate, the austenite can transform to martensite and a final microstructure of different levels of ferrite and martensite (the typical microstructure of dual-phase steels) can be accomplished. Due to their composite microstructures (ferrite and martensite), dual-phase steels exhibit excellent mechanical properties with ultimate tensile strengths (UTS) generally dependent primarily on the volume fraction of martensite. These steels are therefore classified according to their ultimate tensile strength; for example, DP500 has a UTS of approximately 500 MPa while DP1000 would have an approximate UTS of 1000 MPa.

Because of the successful use of this alloy in MBJ and, particularly since it was seen that the material was able to achieve high sintered densities (> 7.5 g/cm^3) despite the very low as built densities of the MBJ process (< 4.5 g/cm^3), it was decided to explore this alloy for use in MIM. The physical characteristics and chemical analysis of the powder used in this study are shown in Table I.

Table I: Powder properties of Air Melted- Gas Atomized FSLA. Chemical composition shown in weight percent.

	Apparent Density	Tap Density	Carbon	Sulfur	Oxygen	Nitrogen	d_{10}	d_{50}	d_{90}
Material	**g/cm^3**	**g/cm^3**	**wt.%**	**wt.%**	**wt.%**	**wt.%**	**Micrometers**	**Micrometers**	**Micrometers**
FSLA Powder	3.2	4.9	0.14	0.007	0.06	0.01	5.7	14.0	24.4

Material	Mn	Cr	Ni	Mo	Nb	V	Si
FSLA Powder	0.20	1.60	0.06	1.45	0.18	0.18	1.64

EXPERIMENTAL PROCEDURE

Powders utilized in this study were air melted and gas atomized with nitrogen. Chemical analysis and powder properties are listed in Table I.

All MBJ test samples were printed on an HP Multi Jet Fusion Printer, with a water-based binder at a 50-micrometer layer thickness.[4]

For MIM produced samples, two binder systems were utilized: ADVACAT® and ADVAMET® both supplied by Advanced Metalworking Practices (AMP). The ADVACAT® system is a catalytic binder system while the ADVAMET® is a polymeric binding system.[5] Tensile specimens were molded on an Arburg molding machine. Catalytic and polymeric debinding were performed by DSH Technologies and weight loss measurements were made prior to sintering to ensure proper debinding.

Test pieces were sintered at DSH Technologies utilizing MIM3045T furnaces from Elnik Systems. These furnaces combine the thermal debind and the sinter processes in one furnace. The equipment has a maximum temperature of 1600 ^{o}C with partial pressure or vacuum control. The furnace has an all-metal process zone with atmosphere capabilities of pure hydrogen, nitrogen, argon, or vacuum environments. For this study, the test pieces were sintered in a high temperature Elnik MIM at 1380 ^{o}C for 30 minutes in an atmosphere of 95 vol.% nitrogen / 5 vol.% hydrogen.

For continuous heat treatment, a high temperature Abbott continuous-belt furnace was used at the indicated temperatures for 30 minutes in an atmosphere of 95 vol.% nitrogen / 5 vol.% hydrogen.

Prior to mechanical testing, green and sintered densities, dimensional change (DC), and apparent hardness were determined on the tensile and transverse rupture (TR) samples. For the MBJ samples five tensile specimens (flat dogbones/unmachined) and five TR specimens were evaluated for each composition. The densities of the green and sintered steels were determined in accordance with MPIF Standard 42. Tensile testing followed MPIF Standard 10 and apparent hardness measurements were made on the tensile and TR specimens, in accordance with MPIF Standard 43. For the MIM process, standard MIM tensile bars were produced according to MPIF Standard 50.

Porosity measurements were made on metallographically prepared cross-sections removed from entire test parts. A Clemex automated image analysis system was used to measure and map the porosity on as-prepared surfaces using a predetermined gray level to separate the dark void space and from the highly light reflective metallic regions. This provided the opportunity to estimate the pore content in both the sample volume and in localized regions.

Specimens for microstructural characterization were prepared using standard metallographic procedures. Subsequently, they were examined by optical microscopy in the polished and etched (2 vol.% nital / 4 wt.% picral) conditions.

In addition, the microstructure was revealed and color was used to separate the transformation products with a two-step, etch/stain, process. First, the microstructure was defined with a light pre-etch by immersing the sample in Vilella's Reagent (5 mL HCl + 1 g picric acid + 100 mL ethyl alcohol), rinsing with warm water, and drying with filtered compressed air. In the second step, the pre-etched sample was immersed in a freshly prepared solution of 10 g sodium metabisulphite (Na2S2O5) in 100 mL deionized or distilled water, rinsed with warm water and alcohol, then dried with filtered compressed air. This was utilized to highlight the dual phase microstructure in the material (ferrite and martensite/bainite).

RESULTS AND DISCUSSION

One of the major differences between MBJ and MIM is the starting density and porosity distribution in the specimen prior to sintering. In MBJ, since the powders are built layer-by-layer with very little force imposed by the spreading device (called the re-coater), the powder density

in the as-built compact is often not much greater than the apparent density of the powder. In addition, because the specimen is built layer-by-layer, there is often a directionality to the layers that can sometimes lead to areas of porosity in between the layers. Typical as-built densities are in the range of 4.5 g/cm^3. With MIM, the metal powder/binder slurry is injected into the die cavity using pressure and heat resulting in a specimen with higher density and a more even porosity distribution. Densities in MIM are typically 1 g/cm^3 higher than in MBJ prior to the sintering process. Stereoscope and SEM pictures documenting the level and distribution of porosity are shown in Figure 1.

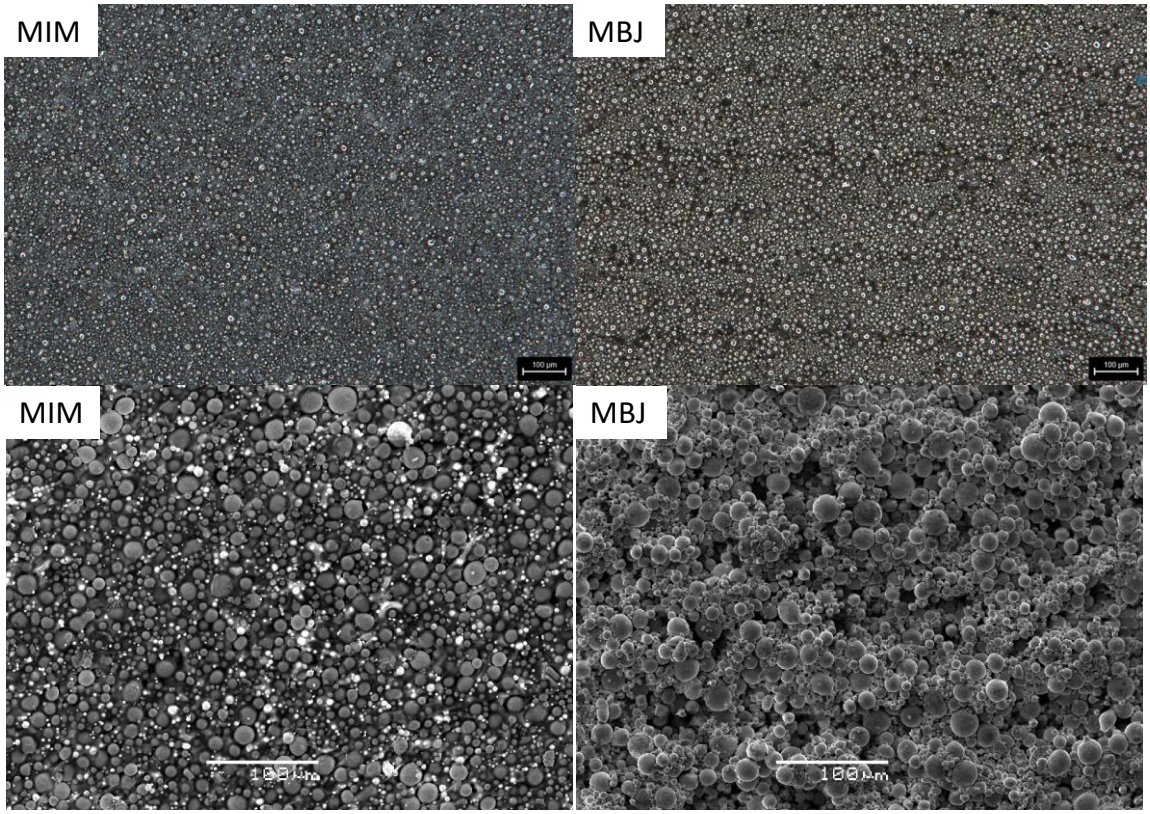

Figure 1: Stereoscope images (top) and Scanning Electron Microscopic Images (bottom) of MIM as built samples (left) versus as printed samples of MBJ (right) showing formation of porosity during building process.

As mentioned previously, the FSLA alloy was designed to sinter at a temperature where there were equal amounts of ferrite and austenite. The ferrite having a more open crystal structure versus the austenite [body centered cubic (BCC) versus face centered cubic (FCC)] is one factor that leads to better diffusion and, hence, better sintered densities. In addition, the amount of grain boundaries between the two phases also contributes to a higher diffusion rate when compared to single phase microstructures. In previous work, even though the as-built density (or green density) of the MBJ was fairly low, the sintered density was greater than 97% of the pore-free density. With MIM, considering the higher as-built density, one would assume the sintered density and therefore the mechanical properties of the MIM FSLA would be slightly higher than

the FSLA samples produced from MBJ-processed samples under the same conditions. However, one must also consider potential interactions of the binders with the FSLA alloy. The binder used in MBJ seemed to have no negative effect on the FSLA alloy produced with that process but the two types of MIM binders (catalytic and polymeric) still needed to be examined.

Table II: Mechanical Properties and microstructural characteristics of as sintered specimens. Sintered in 95 vol.% nitrogen / 5 vol.% hydrogen atmosphere at 1380 ºC

Condition	UTS [MPa]	0.2%YS [MPa]	Elong [%]	Hardness [HRA]	Porosity [%]	Ferrite [%]
MBJ	712	393	10.1	55	2.68	81
MIM Catalytic	838	469	17.1	56	1.63	84
MIM Polymeric	859	482	16.5	56	0.46	82

Table II shows the results of the mechanical properties of specimens produced by the MIM (different binders) and MBJ. The two MIM materials have higher densities than the MBJ specimens and this leads to better strengths and elongations. This is not surprising as the starting density of the MBJ samples are so much lower than the MIM produced samples. The ductility of the MBJ samples is substantially lower than the MIM samples despite the fact that the microstructures of the samples are very similar. Metallographic systematic point counts of the phases present in the three different materials indicate that they are all roughly 80% ferrite and 20% bainite. The sintered carbon of the samples was all the same at 0.11 wt.% and, since they were all sintered under the same conditions, the cooling rate led to the same as-sintered microstructure (Figure 2). Examining the microstructure of the MBJ samples in Figure 2, it is evident that the porosity is not only greater than the MIM samples, but also has directionality which, in this case, was nearly perpendicular to the tensile axis. This is supposed to be the reason for the low ductility of the MBJ produced samples.

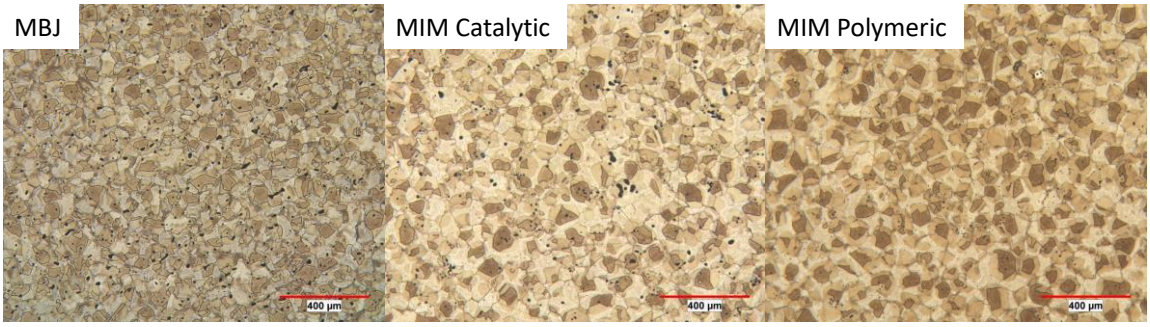

Figure 2: Optical Microstructures of FSLA produced by MBJ and MIM (catalytic and polymeric binders). Sintered in 95 vol.% nitrogen / 5 vol.% hydrogen atmosphere at 1380 ºC.

One of the unique features of the FSLA alloy is the wide range of temperatures in which the alloy can be heat treated in the two-phase region of austenite and ferrite. This is shown by the diagram produced from the thermodynamic software package, CALPHAD, in Figure 3.[6] When heat treated at a temperature of approximately 870 ºC, the microstructure of the FSLA

alloy contains greater than ~95% ferrite. Conversely, when held at temperatures near 1150 °C the microstructure is ~ 90% austenite, which can transform to either bainite or martensite depending on the cooling rate. One of the key features of dual-phase steels is the ability to vary the mechanical properties by changing the levels of martensite and ferrite.[7-8] If a material of higher strength and hardness is required, intercritical annealing is performed at a temperature at which there is a high level of austenite that can transform to a harder and stronger phase during cooling. If a material with lower strength but better ductility is required, an intercritical annealing temperature which favors the formation of the softer, stable ferrite phase is chosen. In order to evaluate the range of properties the FSLA alloy could exhibit, it was decided to test the extreme differences into the effects of the two phases. Consequently, samples that were ~ 90% stable ferrite and samples that were 90% austenite, with the ability to transform to bainite or martensite depending on the cooling rate, were heat treated.

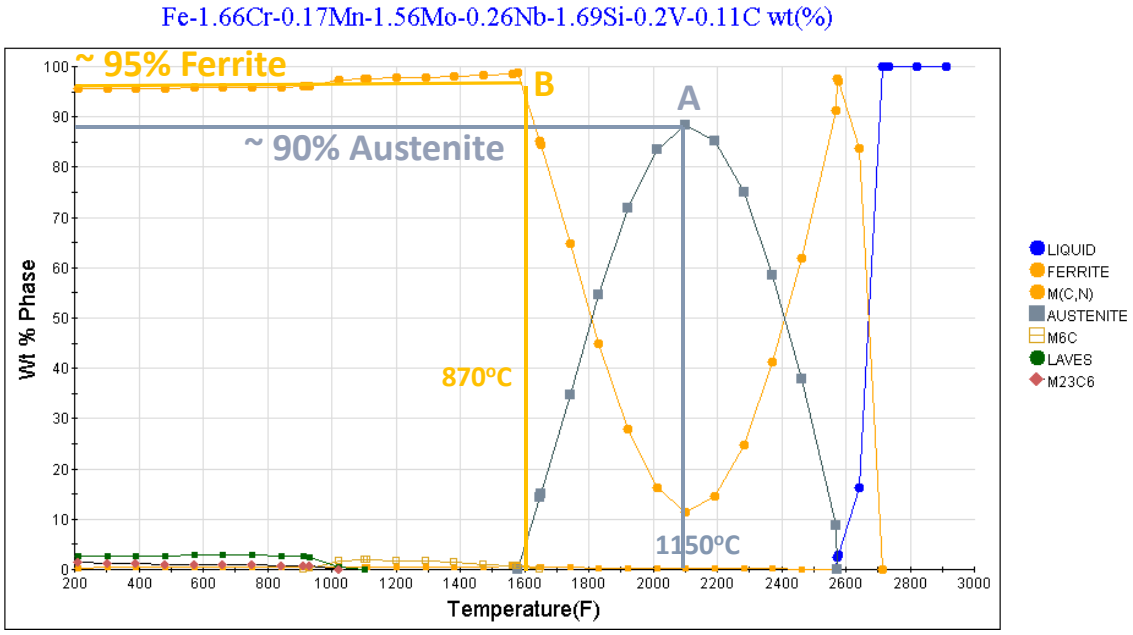

Figure 3: CALPHAD generated diagram for the phases present at various temperatures for the FSLA alloy chemical composition shown in Table II.

However, using the equilibrium-diagram in Figure 3 does not account for the kinetics of the phase transformations to take place. The initial microstructure of the test specimens that exists after sintering and subsequent cooling from the sintering temperature is a mixture of transformation products (martensite/bainite) and ferrite. When the test specimens are heated to 1200 °C, both the harder transformation products and the ferrite need to change structure to new proportions of austenite and ferrite. This is done by the time driven event of partitioning of elements. In order to evaluate the amount of time needed to compete the transformations sintered samples of the MBJ FSLA were heat treated for 1-5 hrs. at 1200 °C in a vacuum furnace under a partial pressure of nitrogen. Tensile properties and hardness values were measured after each of the time increments. In addition, quantitative metallography was used to determine the level of martensite in the specimens. The ultimate tensile strength and hardness values reached a maximum at a time between 4-5 hours eventually, achieving a UTS of 1050 MPa. Therefore, it was decided to also heat treat the MIM produced samples for 5 hours at 1200 °C.

Table III: Mechanical Properties and microstructural characteristics of heat treated at 1200 °C for 5 hours.

Condition	UTS [MPa]	0.2%YS [MPa]	Elong [%]	Hardness [HRA]	Porosity [%]	Bainite [%]
MBJ	1054	650	12.9	58	3.38	83
MIM Catalytic	1023	616	12.5	62	1.57	61
MIM Polymeric	970	561	11.8	60	0.56	64

A comparison of the effect of this heat treatment is shown in Table III. Since the microstructure of all samples had more transformation products (bainite) than the as-sintered specimens, the ultimate tensile strength was significantly higher in all the samples. This was the desired effect as heat treating at 1200 °C allowed for diffusion of the alloying elements, most notably carbon, chromium, silicon and molybdenum. Carbon, which diffuses interstitially, has the biggest impact since it has both the greater mobility and also is the most effective element in hardening the bainite as it transforms from the high temperature austenite. Examination of Figure 3 shows that the maximum amount of transformation products (slightly to the right of point A) that can form is approximately 85% based on the amount of austenite present at 1200 °C. The quantitative metallography in Table III shows that the MBJ sample was able to obtain close to this value while in both of the MIM samples, only approximately 60% transformation occurred. This resulted in a lower UTS strength of the material despite their higher density (lower porosity). The mechanism for this is unclear but is supported by the microstructures shown in Figure 4. Since the MIM and MBJ samples were sintered at different times, it is possible that a variation in the cooling rate occurred. In addition, the standard MIM tensile bars have a lower cross sectional area than the flat dogbone tensile bars used in MJB, and the time at temperature may have been different for the two different types of samples. Since all the development of the heat treat cycle was based on the MBJ samples this will be re-examined in future work to improve the MIM heat treatment procedure. However, key to this study is that the heat treatment at 1200 °C dramatically increased the strength of the material from the as-sintered condition. Having one material which can be heat treated to several different property levels shows the utility of the alloy design.

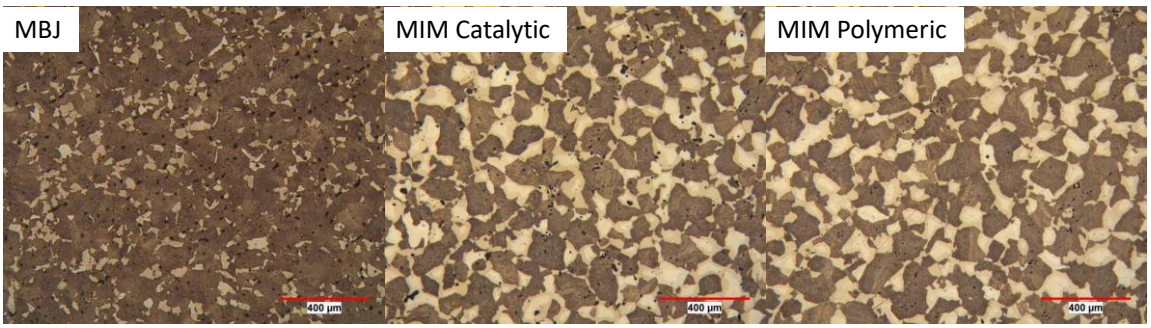

Figure 4: Optical Microstructures of MBJ FSLA and MIM FSLA (catalytic and polymeric binders). Sintered in 95 vol.% nitrogen / 5 vol.% hydrogen atmosphere at 1380 °C then heat treated for 5 hrs. at 1200 °C.

Another set of experiments were conducted in which the FSLA was intercritically annealed in a range of 800-900 ºC. At this temperature, the indication from Figure 3 (Point B) is that the microstructure of the alloy will be predominantly ferrite, which will allow for a material with much higher level of ductility. This increase in ductility (elongation) is useful in the sheet metal components in the automotive industry where the energy from impact needs to be absorbed (mainly the chassis area such as bumpers).[9] The microstructure of the FSLA alloy after the sintering process is a mixture of ferrite and some transformation products (usually bainite). Therefore, it was necessary to reheat the samples, allowing the already transformed ferrite (from sintering) to transform to austenite and allowing for a maximum amount of ferrite to be formed by holding at this temperature. For this reason, the samples were heated for 1 hour at 1200 ºC followed by a furnace cool to an intercritical anneal temperature at of 800 ºC for 2 hrs.

Table IV: Mechanical Properties and microstructural characteristics of heat treated at 1200 ºC for 1 hrs. furnace cooled to 800 ºC and held for 2 hrs. followed by furnace cooling to room temperature.

Condition	UTS [MPa]	0.2%YS [MPa]	Elong [%]	Hardness [HRA]	Porosity [%]	Ferrite [%]
MBJ	604	326	23.0	49	2.51	87
MIM Catalytic	610	330	21.7	44	1.5	100
MIM Polymeric	673	361	23.3	51	0.63	100

The mechanical properties shown in Table IV show all the materials had a high level of ductility. The two MIM produced specimens, as with the other samples in this study, showed a higher density and, as a result of this heat-treatment, the ferrite was maximized and the MIM with the polymeric binder had a significantly higher strength while maintain the high ductility (> 23%).

Holding at these temperatures allowed for the reformation of the high temperature austenite to stable ferrite from the redistribution of alloying elements. In order to maximize ductility, there is a necessity to balance the level of ferrite which predominates at the lower temperatures (800 ºC) with the amount of carbide formation from elements like niobium, vanadium and molybdenum which are contained in the alloy (Table I). The precipitates that form from these elements were useful in creating the high strength necessary in higher bainitic alloys, but hinder dislocation motion and therefore limit the ductility of the alloy at the range necessary to achieve the high elongation values achieved in this heat-treatment. Figure 5 shows that with this heat treatment the microstructure was predominantly ferrite for all the materials. Interestingly, the MIM produced samples seemed to have a lower percentage and size of the carbides in the material.

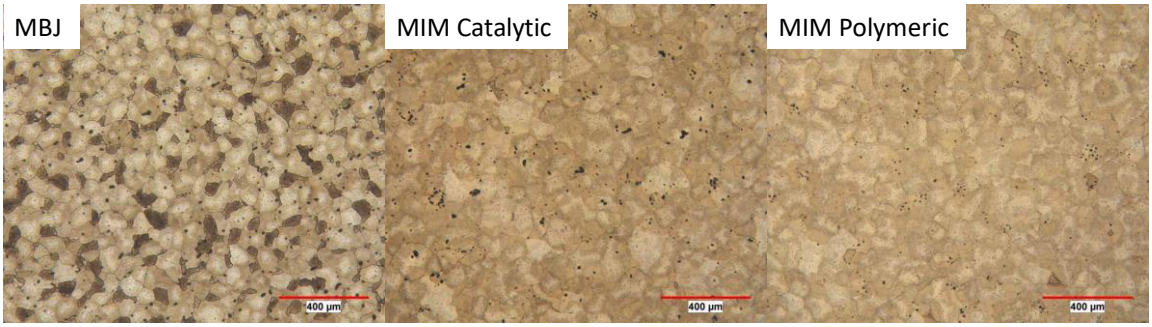

Figure 5: Optical Microstructures of MBJ FSLA and MIM FSLA (catalytic and polymeric binders). Sintered in 95 vol.% nitrogen / 5 vol.% hydrogen atmosphere at 1380 ºC then heat treated for 1 hr. at 1200 ºC then furnace cooled to 825 ºC and held for 2 hrs. then furnace cooled.

SUMMARY AND CONCLUSIONS

It is apparent from the previous discussion that the FSLA alloy properties can be varied significantly by the manner in which it is heat treated after sintering. The alloy was initially developed as a replacement for a wrought DP600, which acquires its dual-phase microstructure and mechanical properties through a combination of controlled rolling and intercritical annealing heat treatments. But in addition to the DP600, there are a range of DP alloys used in conventional wrought processing that have a range of ultimate tensile strengths ranging from 480 MPa to 1050 MPa.[10] In many cases, this is accomplished by increasing the carbon level to the same base alloy chemistry. However, in the FSLA alloy, a wide range of microstructure proportions (transformation products and ferrite) can be achieved by changing the intercritical annealing temperature, with the additional benefit of varying the amount and size of the precipitated carbides, leading to a very flexible alloy in terms of mechanical properties. This is highlighted in Figure 5, where elongation versus ultimate tensile strength of the wrought versions of dual-phase alloys (DP450, D490, DP590, DP780 and DP980) and the FSLA alloy made by MBJ and MIM (combined data of catalytic and polymeric binders) are plotted for a range of different heat treatments. In the FSLA alloys, only the heat treatment is adjusted to tailor the mechanical properties therefore saving a significant amount of development time in the forming process. The MIM produced FSLA shows significantly higher properties than the wrought material over the range of ultimate tensile strengths examined. The MIM produced FSLA also shows improvements over the MBJ produced FSLA for the low to medium range of strengths while showing improved densities over the MBJ for all cases. While close in strength at the higher UTS levels to the MBJ, further development is needed to obtain the higher level of transformation product in the final microstructure. Also shown in this study is the fact that the MIM binders utilized are suitable for the FSLA powder, but the polymeric based binder had higher overall densities.

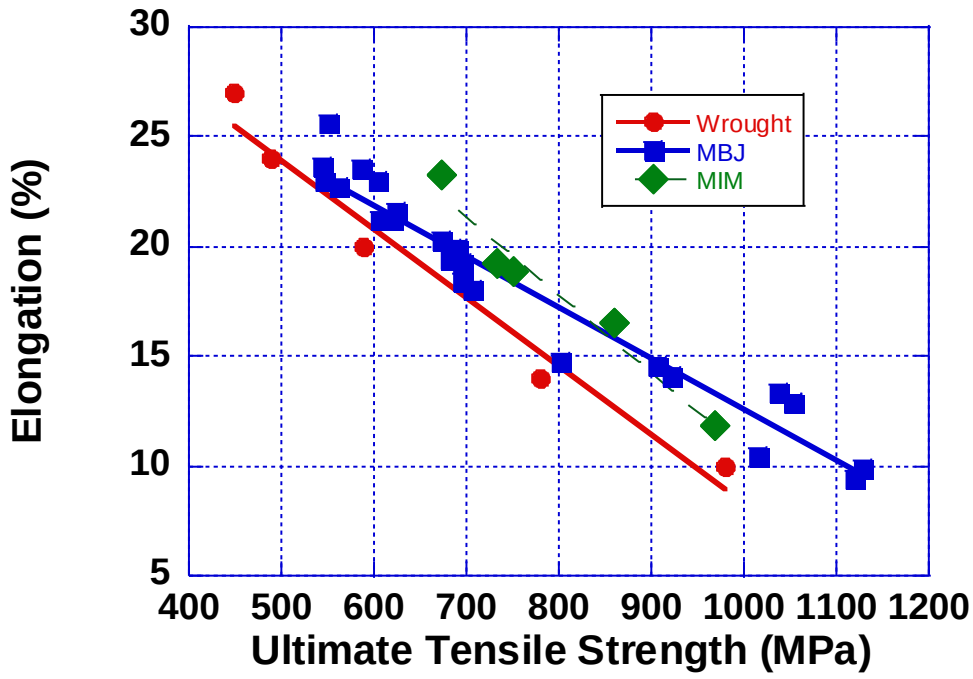

Fig. 6: Mechanical properties of FSLA after different heat treatments. Includes MIM,MBJ and Wrought grades of Dual Phase Steels.

The FSLA material has shown good promise for use in MIM, and further development is warranted as additional heat treatments still need to be explored. Particularly interesting is the wide range of material properties that can be achieved with one material without changing the injection and sintering process. The heat treatments proposed are simple and easily applied in practice.

REFERENCES

1. C. Schade, T. Murphy, K. Horvay, A. Lawley and R. Doherty, Development of a Free Sintering Low Alloy (FSLA) Steel for the Binder jet Process, *Advances in Additive Manufacturing with Powder Metallurgy – 2021*, compiled by S. Atre and S. Jackson, Metal Powder Industries Federation, Princeton, NJ, 2021, part 7 pp.287-306.
2. N.B. Shaw and R.W.K. Honeycombe, “Some Factors Influencing the Sintering Behaviour of Austenitic Stainless Steels,” Powder Metallurgy, 1977; vol. 20: pp. 191-198.
3. R.I. Sands and J.F. Watkinson, “Sintered Stainless Steels I.- The influence of Alloy Composition upon Compacting and Sintering Behaviour,” Powder Metallurgy, 1960, No. 5, pp.85-104.
4. HP. Inc. Technical White Paper, “HP Metal Jet Technology,” 2018, www8.hp.com/h20195/v2/GetPDF.aspx
5. https://ampmim.com/feedstock
6. https://calphad.org/

7. C.C. Tasan, M. Diehl, D. Yan, M. Bechtold, F. Roters, L. Schemmann, C. Zheng, N. Peranio, D. Ponge, M. Koyama, K. Tsuzaki, D. Raabe, An Overview of Dual-Phase Steels: Advances in Microstructure-Oriented Processing and Micromechanically Guided Design, Annu. Rev. Mater. Res. 45 (2015) 391–431.
8. R.A. Kot and B.L. Bramfit, Editors, “Fundamentals of Dual Phase Steel,” The Metallurgical Society of AIME, 1981.
9. World Steel Auto Future Steel Vehicle Overview Report-2011. http://www.worldautosteel.org/download_files
10. Voest Alpine Product Data Sheet for Dual Phase Steels, June 2019, page 3. https://www.voestalpine.com/stahl/en/content/